



ISSN: 0067-2904

The Effects of Electrical Conductivity on Fluid Flow between Two Parallel Plates in a Porous Medium

Alaa Hammodat*, Ghanim Algawuish, Iman Al-Obaidi

Department of Mathematics, College Education of Pure Science, Mosul University, Nineveh, Iraq

Received: 19/9/2021

Accepted: 30/10/2021

Abstract

This paper deals with a mathematical model of a fluid flowing between two parallel plates in a porous medium under the influence of electromagnetic forces (EMF). The continuity, momentum, and energy equations were utilized to describe the flow. These equations were stated in their nondimensional forms and then processed numerically using the method of lines. Dimensionless velocity and temperature profiles were also investigated due to the impacts of assumed parameters in the relevant problem. Moreover, we investigated the effects of Reynolds number \mathcal{R}_e , Hartmann number M , magnetic Reynolds number \mathcal{R}_m , Prandtl number \mathcal{P}_r , Brinkman number \mathcal{F}_s , and Bouger number ω , beside those of new physical quantities (N , \mathcal{H}). We solved this system by creating a computer program using MATLAB.

Keywords: Heat transfer, Porous media, Hartmann number, Magnetic Reynolds number, Prandtl number, Reynolds number.

تأثير التوصيلية الكهربائية على تدفق السوائل بين لوحين متوازيين في وسط مسامي

علاء حمودات* ، غانم الجاويش ، ايمان العبيدي

قسم الرياضيات، كلية التربية للعلوم الصرفة، جامعة الموصل، نينوى، العراق

الخلاصة

يتناول هذا البحث نموذجاً رياضياً لسائل يتدفق بين لوحين متوازيين في وسط مسامي تحت تأثير القوى الكهرومغناطيسية (EMF). المعادلات التي استخدمت لوصف هذا الجريان هي معادلات الاستمرارية والحركة والطاقة وقد تمت كتابة هذه المعادلات من اجل الحصول على الصيغ اللابعدية لكل منها ومن ثم معالجتها عددياً باستخدام طريقة (Method of Line). وبيننا ان تأثير المسالة في السرعة ودرجة الحرارة اللابعدية عن طريق المعلمات المفترضة. بالإضافة الى ذلك، وجدنا تأثير عدد رينولد \mathcal{R}_e ، عدد هارتمان M ، عدد رينولد المغناطيسي \mathcal{R}_m ، عدد برانتدل \mathcal{P}_r ، عدد برنكمان \mathcal{F}_s ، عدد بوجر ω الى جانب الكميات الفيزيائية الجديدة N ، \mathcal{H} . حللنا هذا النظام بواسطة برنامج حاسوبي باستخدام MATLAB.

1. Introduction

Because of its vital applications in sciences that influence human life, the flow of electrically directed liquids across porous parallel plates has become a major issue. This is evident in food industry, extraction of crude oil from the earth, and the movement of the blood [1]. Several researchers have looked at transferring the flow of oscillator liquids

*Email: alaahammodat@uomosul.edu.iq

between two parallel plates in various magnetic fields. Under saturated temperature conditions, Makinde and Mhone [2] used the combined effects of a random magnetic field and thermal radiation transmission to describe the unstable flow of high-optical fluid connected through a tube filled with irregular porous walls.

For the magneto hydrodynamic (MHD) oscillatory flow of Williamson fluid across a porous plate, Khudair and Al- Khafajy [1] devised a heat transfer model for two types of flow (Couette flow and Poiseuille flow). Al- Khafajy [3] studied the effects of magneto hydrodynamic (MHD) oscillatory slip flow of Jeffrey fluid with varying viscosity, temperature, and concentration, on a porous plate. Hanvey *et al.* [4] studied the effects of an inclined magnetic field, as well as heat and mass transmission, on two infinite parallel plates using porous materials. The differential transformation method was used by Sheikholeslami *et al.* to investigate the problem of unstable nanofluid flow between parallel plates [5].

In the presence of an inclined magnetic field, , as well as radiative heat flux and heat source, Mehta *et al.* [6] explored oscillatory fluid flow and heat transfer via a porous material between parallel plates. Mukhopadhyay and Mandal [7] looked for numerical solutions for steady state MHD mixed convective boundary layer flow and heat transfer through a porous plate in the presence of velocity and thermal slips. Kumari and Gayal [8,9] demonstrated the effects of mass transfer, viscous suction parameter, and the dissipative impact on a two-dimensional steady-state hydromagnetic viscous fluid flow between two parallel plates in the presence of heat radiation. The steady state three-dimensional MHD flow of fluid injected uniformly into the vertical channel with porous wall through one side of the channel was solved analytically by Jabr and Abdulhadi [5]. Our goal here is to investigate the flow of fluids in a cross-section under the influence of an electromagnetic field (EMF) and use the method of lines to solve the partial differential equations that describe the situation. In addition, we aim to demonstrate the behavior of temperature within the cross-section and the impacts of physical quantities.

2. Research Method

In the following sections, we try to solve our main equations in a simple way using a dimensionless approximation, after defining the model under study and the equations that control it in addition to the boundary conditions of the problem.

2.1. Protection Equation

We consider the magnetic fluid through a porous medium moving between two horizontally parallel plates with a distance of h^* and a cross-section length of l^* (Figure1). The model described by the cartesian coordinate system with x coordinate is parallel to the channel wall in the flow direction and the y coordinate is in the channel's vertical direction. The magnetic field \mathcal{B} utilized across the channel is parallel to the y -axis, with a component parallel to the y -axis is fixed and symbolized as \mathcal{B}_0 . The component in the x -axis direction is \mathcal{B}_x , which inflows along the channel in the flow direction, while the component in the z -axis direction is equal to zero.

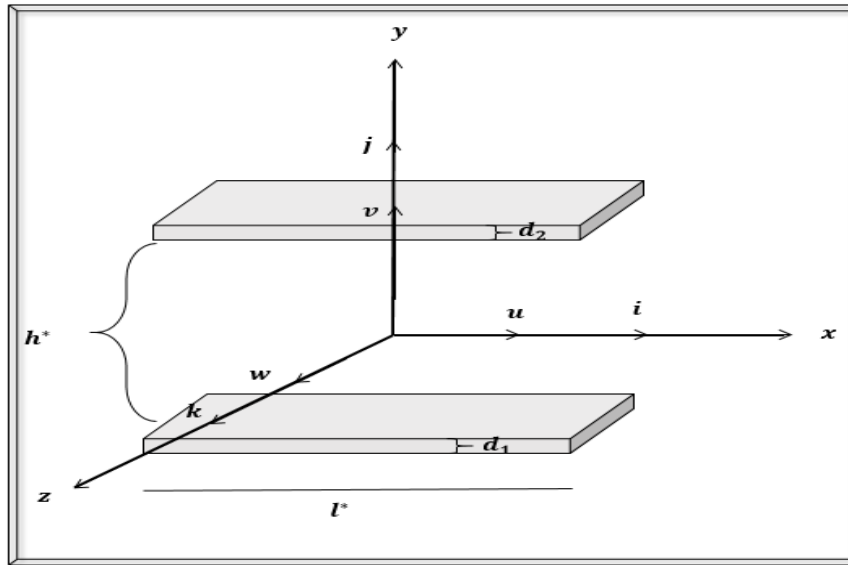


Figure 1- Physical Model and System of Coordinates.

The fundamental governing equations, consisting of the mass conservation, momentum, and energy equations, are given by:

The continuity equation is

$$\frac{\partial u^*}{\partial x^*} + \frac{\partial v^*}{\partial y^*} = 0 \tag{1}$$

The momentum equations are:

in the x direction:

$$\frac{\partial u^*}{\partial t^*} + u^* \frac{\partial u^*}{\partial x^*} + v^* \frac{\partial u^*}{\partial y^*} = -\frac{1}{\rho^*} \frac{\partial p^*}{\partial x^*} + \nu^* \left[\frac{\partial^2 u^*}{\partial x^{*2}} + \frac{\partial^2 u^*}{\partial y^{*2}} \right] - \frac{\nu^*}{K^*} u^* + \frac{1}{\rho^* \mathcal{M}_e} \left[B_0 \frac{\partial B_{x^*}}{\partial y^*} \right] \tag{2}$$

in the y direction:

$$\frac{\partial v^*}{\partial t^*} + u^* \frac{\partial v^*}{\partial x^*} + v^* \frac{\partial v^*}{\partial y^*} = -\frac{1}{\rho^*} \frac{\partial p^*}{\partial y^*} + \nu^* \left[\frac{\partial^2 v^*}{\partial x^{*2}} + \frac{\partial^2 v^*}{\partial y^{*2}} \right] - \frac{\nu^*}{K^*} v^* + \frac{1}{\rho^* \mathcal{M}_e} \left[B_{x^*} \frac{\partial B_{x^*}}{\partial y^*} \right] + \rho^* g^* \tag{3}$$

The heat equation is:

$$\rho^* C_v^* \left[\frac{\partial T^*}{\partial t^*} + u^* \frac{\partial T^*}{\partial x^*} + v^* \frac{\partial T^*}{\partial y^*} \right] = \kappa^* \left[\frac{\partial^2 T^*}{\partial x^{*2}} + \frac{\partial^2 T^*}{\partial y^{*2}} \right] - \left[\frac{\partial q_{x^*}^*}{\partial x^*} + \frac{\partial q_{y^*}^*}{\partial y^*} \right] + \frac{1}{\sigma^* \mathcal{M}_e^2} \left[\frac{\partial B_{x^*}}{\partial y^*} \right]^2 \tag{4}$$

In these equations, (u^*, v^*) are the velocity of axial motion, (ρ^*) is the density, (p^*) is the pressure, ν^*

is the kinematic viscosity, K^* is the permeability of medium, (\mathcal{M}_e) is the agnetic permeability of medium, (\vec{B}) is the magnetic field vector, (B_{x^*}, B_0) is the magnetic field component in x^* and y^* directions, respectively, g^* is a gravitational acceleration constant, C_v^* is the specific heat at constant volume, κ^* is the thermal conductivity coefficient, T^* is the temperature, and $q_{x^*}^*, q_{y^*}^*$ are the components of radiation in the x^* and y^* directions, respectively.

The associated boundary conditions applied on the top and the bottom of the model are:

$$\left. \begin{aligned}
 u^* = v^* = 0 & \quad \text{at } y^* = 0, h^* \\
 T^* = T_1^* & \quad \text{at } y^* = 0 \\
 T^* = T_2^* & \quad \text{at } y^* = h^* \\
 \frac{\partial T^*}{\partial x^*} = 0 & \quad \text{at } x^* = 0, l^* \\
 \frac{\partial B_{x^*}}{\partial y^*} - \frac{\sigma^*}{\sigma_1^* d_1} B_{x^*} = 0 & \quad \text{at } y^* = 0 \\
 \frac{\partial B_{x^*}}{\partial y^*} + \frac{\sigma^*}{\sigma_2^* d_2} B_{x^*} = 0 & \quad \text{at } y^* = h^*
 \end{aligned} \right\} \quad (5)$$

2.2. Method of Solution

For the dimensionalization of the governing equations, we adopt the following characteristic quantities: [10]

$$\left. \begin{aligned}
 u^* = u_0^* u, \quad t^* = \frac{h^*}{u_0^*} t, \quad \vec{B} = B_0 \mathcal{M}_e \sigma^* u_0^* h^* \vec{b}, \quad \vec{\nabla} = h^* \vec{\nabla} \\
 T^* = T_1^* \theta, \quad \vec{q}^* = T_1^{*4} \sigma^* \vec{Q}, \quad x^* = h^* x, \quad y^* = h^* y \\
 v^* = v_0^* v, \quad p^* = \rho^* u_0^{*2} p, \quad I = \frac{c I_1}{\omega T_1^{*4}}
 \end{aligned} \right\} \quad (6)$$

where u_0^* is the velocity of mean flow, $\mathcal{R}_e = \frac{h^* \rho^* u_0^*}{\mu}$ is Reynolds number, $M = B_0 h^* \sqrt{\frac{\sigma^*}{\mu^*}}$ is Hartmann number, $\mathcal{R}_m = \mathcal{M}_e \sigma^* u_0^* h^*$ is the magnetic Reynolds number, $G_r = \frac{\rho^* g^* B h^{*2}}{\mu^* u_0^*}$ is the thermal Gratshof number, $\mathcal{P}_r = \frac{\mu^* C_p^*}{\kappa^*}$ is Prantdle number, $\mathcal{F}_s = \frac{\mathcal{M} u_0^*}{\kappa^* \Delta T^*}$ is Brinkman number, $\gamma = \frac{C_p^*}{C_v^*}$ is the specific heat, and $\mathcal{N} = \frac{v h^*}{\kappa^* \Delta T^*}$ and $\mathcal{H} = \frac{G_r}{\mathcal{R}_e} (T_2^* - T_1^*)$ are new quantities.

By substituting (6) into the equations (1) - (5), we obtain the following non-dimensional equations:

$$\frac{\partial u}{\partial x} + \frac{\partial v}{\partial y} = 0 \quad (7)$$

$$\begin{aligned}
 \frac{\partial u}{\partial t} + u \frac{\partial u}{\partial x} + v \frac{\partial u}{\partial y} \\
 = -\frac{\partial p}{\partial x} + \frac{1}{\mathcal{R}_e} \nabla^2 u - \mathcal{N} u + \frac{M^2 \mathcal{R}_m}{\mathcal{R}_e} \left[b_y \frac{\partial b_x}{\partial y} \right]
 \end{aligned} \quad (8)$$

$$\begin{aligned}
 \frac{\partial v}{\partial t} + u \frac{\partial v}{\partial x} + v \frac{\partial v}{\partial y} \\
 = -\frac{\partial p}{\partial y} + \frac{1}{\mathcal{R}_e} \nabla^2 v - \mathcal{N} v + \frac{M^2 \mathcal{R}_m}{\mathcal{R}_e} \left[b_x \frac{\partial b_x}{\partial y} \right] + E - \mathcal{H} \Theta
 \end{aligned} \quad (9)$$

where $E = \frac{1}{\mathcal{F}_r} + \mathcal{H}$ and $\mathcal{F}_r = \frac{u_0^*}{g^* h^*}$ is Froud number.

By deriving the equation (8) with respect to y and the equation (9) with respect to x, and subtract the resulting equations, the non-dimensional general motion equation can be written as:

$$\begin{aligned} & \frac{\partial}{\partial t} \left[\frac{\partial v}{\partial x} - \frac{\partial u}{\partial y} \right] + \left[\frac{\partial}{\partial x} \left(u \frac{\partial v}{\partial x} + v \frac{\partial v}{\partial y} \right) - \frac{\partial}{\partial y} \left(u \frac{\partial u}{\partial x} + v \frac{\partial u}{\partial y} \right) \right] \\ & = \frac{1}{\mathcal{R}_e} \nabla^2 \left[\frac{\partial v}{\partial x} - \frac{\partial u}{\partial y} \right] - \mathcal{N} \left[\frac{\partial v}{\partial x} - \frac{\partial u}{\partial y} \right] + \dots \\ & \dots + \frac{M^2 \mathcal{R}_m}{\mathcal{R}_e} \left[\frac{\partial}{\partial x} \left(b_x \frac{\partial b_x}{\partial y} \right) - \frac{\partial}{\partial y} \left(b_y \frac{\partial b_x}{\partial y} \right) \right] \\ & \quad - \mathcal{H} \frac{\partial \Theta}{\partial x} \end{aligned} \tag{10}$$

But $u = \frac{\partial \psi}{\partial y}$ and $v = -\frac{\partial \psi}{\partial x}$ are the stream functions [11], then the equation (10) becomes:

$$\begin{aligned} \frac{\partial}{\partial t} \nabla^2 \Psi & = \frac{1}{\mathcal{R}_e} \nabla^4 \Psi - \mathcal{N} \nabla^2 \Psi - \frac{M^2 \mathcal{R}_m}{\mathcal{R}_e} \left[\frac{\partial}{\partial x} \left(b_x \frac{\partial b_x}{\partial y} \right) - \frac{\partial}{\partial y} \left(b_y \frac{\partial b_x}{\partial y} \right) \right] \\ & \quad + \mathcal{H} \frac{\partial \Theta}{\partial x} \end{aligned} \tag{11}$$

Put $\xi = \nabla^2 \Psi$, then,

$$\begin{aligned} \frac{\partial \xi}{\partial t} & = \frac{1}{\mathcal{R}_e} \nabla^2 \xi - \mathcal{N} \xi - \frac{M^2 \mathcal{R}_m}{\mathcal{R}_e} \left[\frac{\partial}{\partial x} \left(b_x \frac{\partial b_x}{\partial y} \right) - \frac{\partial}{\partial y} \left(b_y \frac{\partial b_x}{\partial y} \right) \right] \\ & \quad + \mathcal{H} \frac{\partial \Theta}{\partial x} \end{aligned} \tag{12}$$

$$\begin{aligned} \frac{\mathcal{P}_r \mathcal{R}_e}{\gamma} \left[\frac{\partial \Theta}{\partial t} + u \frac{\partial \Theta}{\partial x} + v \frac{\partial \Theta}{\partial y} \right] \\ = \left[\frac{\partial^2 \Theta}{\partial x^2} + \frac{\partial^2 \Theta}{\partial y^2} \right] - \frac{\mathcal{P}_r \mathcal{R}_e}{\gamma} \left[\frac{\partial Q_x}{\partial x} + \frac{\partial Q_y}{\partial y} \right] + M^2 \mathcal{F}_s \left[\frac{\partial b_x}{\partial y} \right]^2 \end{aligned} \tag{13}$$

But $\nabla \cdot \vec{Q} = 16\omega\Theta - 12\omega$ [10], then the non-dimensional energy equation becomes:

$$\begin{aligned} \frac{\mathcal{P}_r \mathcal{R}_e}{\gamma} \left[\frac{\partial \Theta}{\partial t} + u \frac{\partial \Theta}{\partial x} + v \frac{\partial \Theta}{\partial y} \right] \\ = \left[\frac{\partial^2 \Theta}{\partial x^2} + \frac{\partial^2 \Theta}{\partial y^2} \right] - \frac{\mathcal{P}_r \mathcal{R}_e}{\gamma} [16\omega\Theta - 12\omega] + M^2 \mathcal{F}_s \left[\frac{\partial b_x}{\partial y} \right]^2 \end{aligned} \tag{14}$$

The non- dimensional boundary conditions become:

$$\left. \begin{aligned} u = v = 0 \quad \text{at} \quad y = 0,1 \\ \Theta = 0 \quad \text{at} \quad y = 0 \\ \Theta = 1 \quad \text{at} \quad y = 1 \\ b_x = \mathfrak{K}_1 \epsilon \quad \text{at} \quad y = 0 \\ b_x = \mathfrak{K}_2 \epsilon \quad \text{at} \quad y = 1 \end{aligned} \right\} \tag{15}$$

where $\epsilon = \frac{\partial b_x}{\partial y}$.

2.3. Solution of the Problem

In this section, we try to solve the two-dimensional motion equation (12) with the boundary equation (15) and energy equation (14) using numerical simulation for $0 \leq x \leq L_1$ and $0 \leq y \leq L_2$, where L_1 and L_2 are the arbitrary lengths of the computational domain in the x -direction and y -direction, respectively. We consider the case where coefficients u and v are treated as constants at any time step of the competition [12].

The main equations of the motion and energy, (12) and (14), are solved numerically using the method of lines [13]. We discretise the domain above into $N + 1$ points in x -direction and

$M + 1$ points in y –direction, respectively, where $\Delta x = L_1/N$ and $\Delta y = \frac{L_2}{M}$, using forward and backward finite difference methods, as follows:

$$\xi_{x,ij} = \frac{\xi_{i+1j} - \xi_{ij}}{\Delta x} , \quad \xi_{\bar{x},ij} = \frac{\xi_{ij} - \xi_{i-1j}}{\Delta x} \tag{16}$$

$$\xi_{y,ij} = \frac{\xi_{ij+1} - \xi_{ij}}{\Delta y} , \quad \xi_{\bar{y},i,j} = \frac{\xi_{ij} - \xi_{ij-1}}{\Delta y} \tag{17}$$

Then, keeping the time derivative continuous, the derivatives in equation (12) were discretised as follows:

$$\begin{aligned} \xi_{t,ij} = & \frac{1}{\mathcal{R}_e} \left[\left(\frac{\xi_{i+1j} - 2\xi_{ij} + \xi_{i-1j}}{\Delta x^2} \right) + \left(\frac{\xi_{ij+1} - 2\xi_{ij} + \xi_{ij-1}}{\Delta y^2} \right) \right] - \mathcal{N}\xi_{ij} - \dots \\ \dots - & \frac{M^2\mathcal{R}_m}{\mathcal{R}_e} \left[\frac{\partial}{\partial x} \left(b_x \frac{\partial b_x}{\partial y} \right) - \frac{\partial}{\partial y} \left(b_y \frac{\partial b_x}{\partial y} \right) \right] - \mathcal{H} \left[\frac{\Theta_{i+1j} - \Theta_{i-1j}}{2\Delta x} \right] \quad i = 2, \dots, N, j \\ = & 2, \dots, M \tag{18} \end{aligned}$$

We assume the condition $\xi_x = 0$, then we use this condition to determine the fictitious points for the main equation (12) of $\xi_{t,1}$ and $\xi_{t,N+1}$. In the same way, we discretised the energy equation as:

$$\begin{aligned} \Theta_{t,ij} = & - \left(u_{ij} \frac{\Theta_{i+1j} - \Theta_{i-1j}}{2\Delta x} + v_{ij} \frac{\Theta_{ij+1} - \Theta_{ij-1}}{2\Delta y} \right) + \dots \\ \dots + & \frac{\gamma}{\mathcal{P}_r\mathcal{R}_e} \left[\left(\frac{\Theta_{i+1j} - 2\Theta_{ij} + \Theta_{i-1j}}{\Delta x^2} \right) + \left(\frac{\Theta_{ij+1} - 2\Theta_{ij} + \Theta_{ij-1}}{\Delta y^2} \right) \right] - \dots \\ \dots - & \left(16\omega\Theta_{ij} - 12\omega \right) - \frac{\gamma}{\mathcal{P}_r\mathcal{R}_e} M^2\mathcal{F}_s \left[\frac{\partial b_x}{\partial y} \right]^2 , \quad i = 2, \dots, N, j = 2, \dots, M \tag{19} \end{aligned}$$

3. Results and Discussion

In this section, we present the numerical solutions of a magnetized fluid running through a porous medium between two horizontal plates exposed to a source of disturbance. The finite difference method (forward and backward) was applied to calculate the results of the numerical solutions that were obtained graphically. We obtained the numerical results and illustrations of ordinary differential equations, given by equations (18) and (19), using MATLAB programme (ODE solver), as shown in Figures 2-12. The energy profiles in Figures 2, 5, 6, 7 clearly show that the greater Brinkmann number \mathcal{F}_s , the Bouger number ω , the Prandtl number \mathcal{P}_r , and the relative temperature γ , the closer we get to stability. The effect of Hartmann number M is diverging from the stability for both of the motion and energy, when M and temperature increase (Figures 3 and 10).

In Figures 4 and 8, we observe that the higher the Reynolds number \mathcal{R}_e , the closer to stability in both equations (motion and energy). While (Figure 9) shows that the higher magnetized Reynolds number \mathcal{R}_m , the farther from stability. Finally, Figures 11 and 12 show that the smaller the new quantities of \mathcal{H} and N in the motion equation, the further away it is from stability.

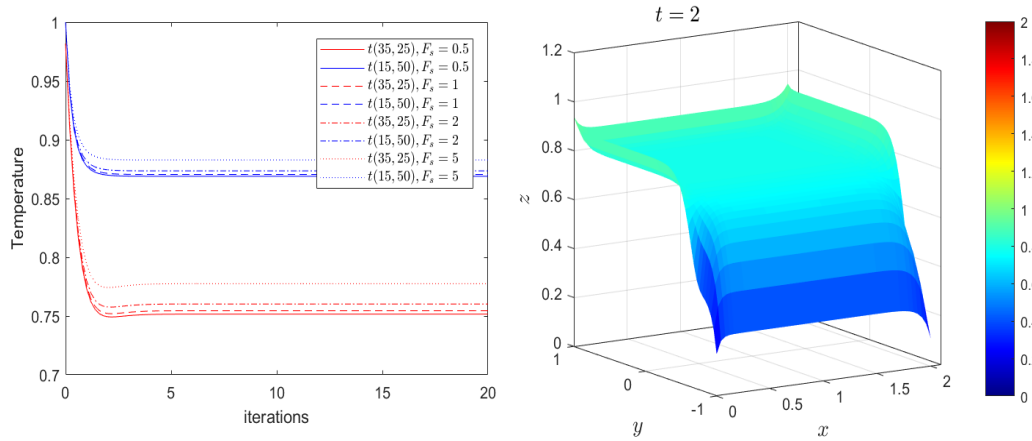


Figure 2 - Effects on the energy equation by varying \mathcal{F}_s (0.5-5) and time (0-20)

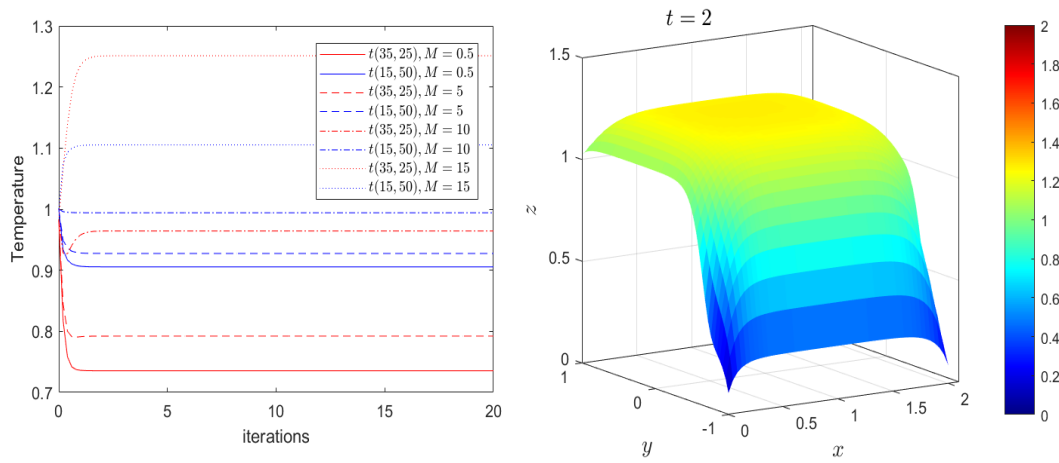


Figure 3 - The energy equation for time $t=0$ to $t=20$ using different values of M ($M=0.5, 5, 10, 15$)

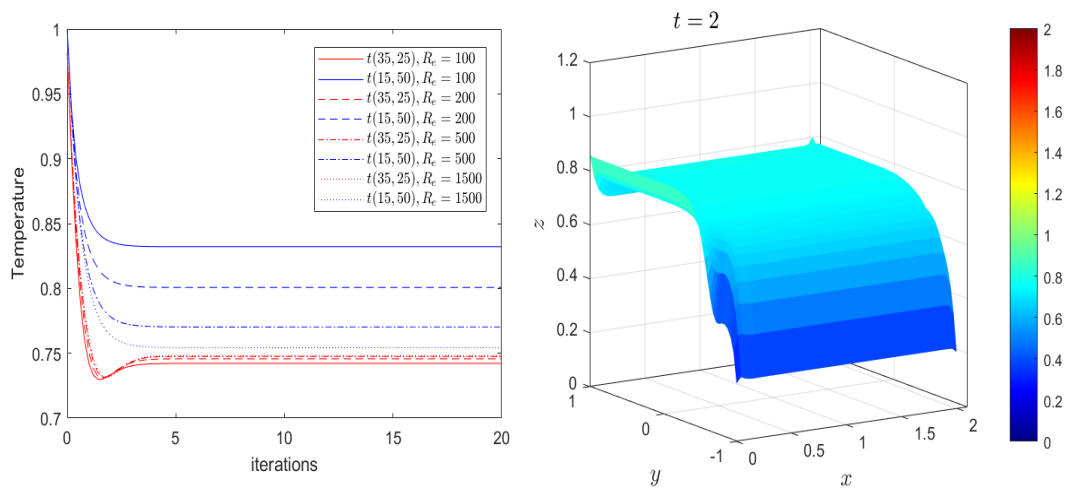


Figure 4 - Effect of \mathcal{R}_e on the energy equation for $t= 0-20$

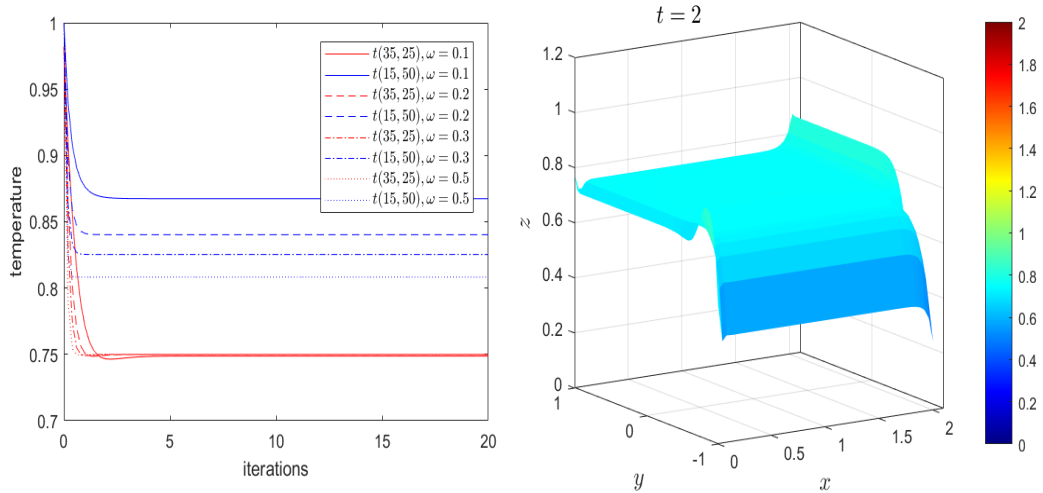


Figure 5 – Effects of varying the number of ω (between 0.1 and 0.5) on energy equation with $t=0-20$

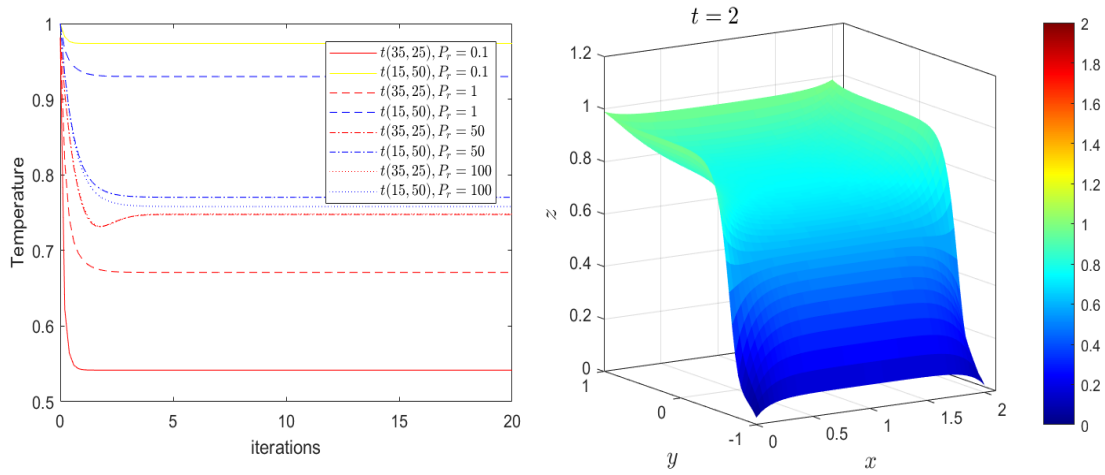


Figure 6 –Impacts of using different values of P_r on energy equation with varying time (from $t=0$ to $t=20$).

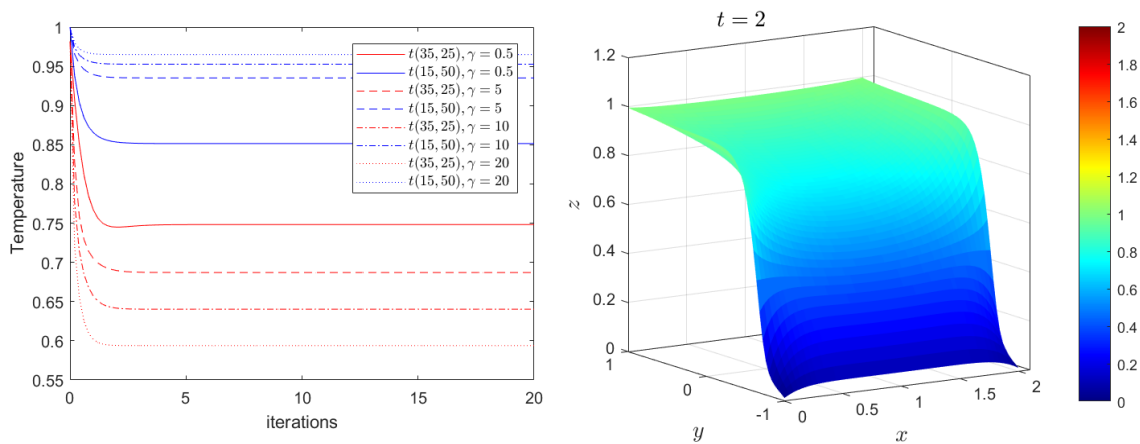


Figure 7 - Impacts of γ , where $\gamma = 0.5,5,10,20$ on the energy equation for $t= 0-20$

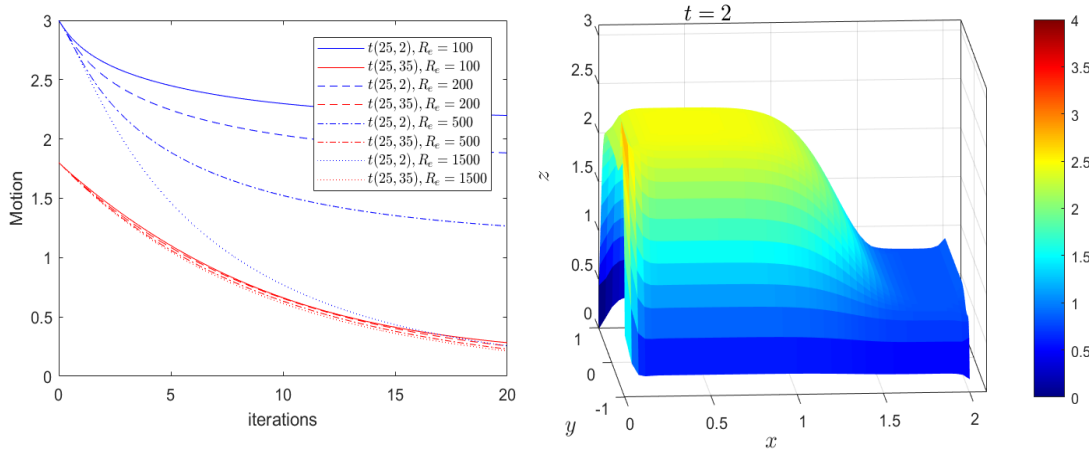


Figure 8 - The motion equation for time $t = 0 - 20$ for varying number of \mathcal{R}_e ($\mathcal{R}_e = 100 - 1500$)

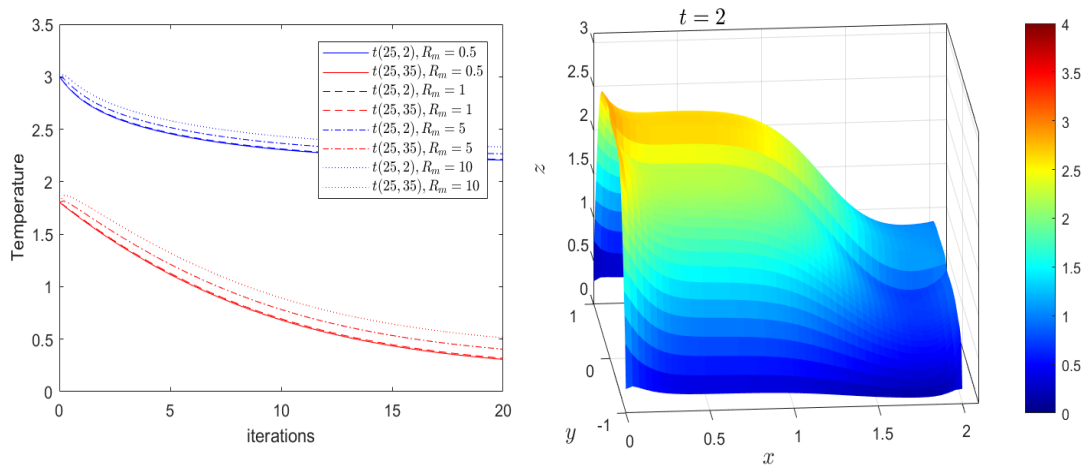


Figure 9 - Influence of varying \mathcal{R}_m number ($\mathcal{R}_m = 0.5, 1, 5, 10$) on the motion equation with time $t = 0 - 20$

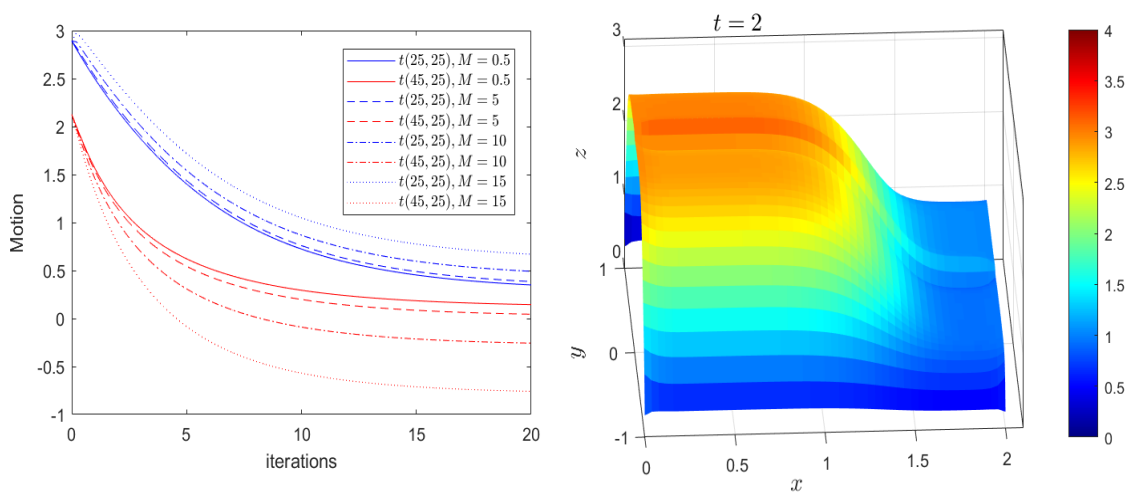


Figure 10 - Effects of varying M between 0.5 and 15 on motion equation

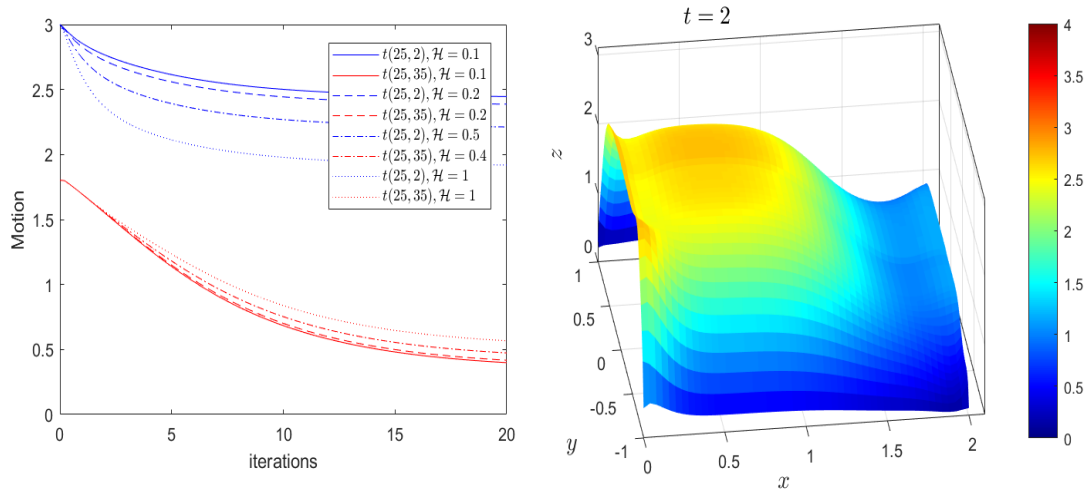


Figure 11 - Effects of varying \mathcal{H} number from $\mathcal{H} = 0.1$ to $\mathcal{H} = 1$ on motion equation for time between $t=0$ to $t=20$

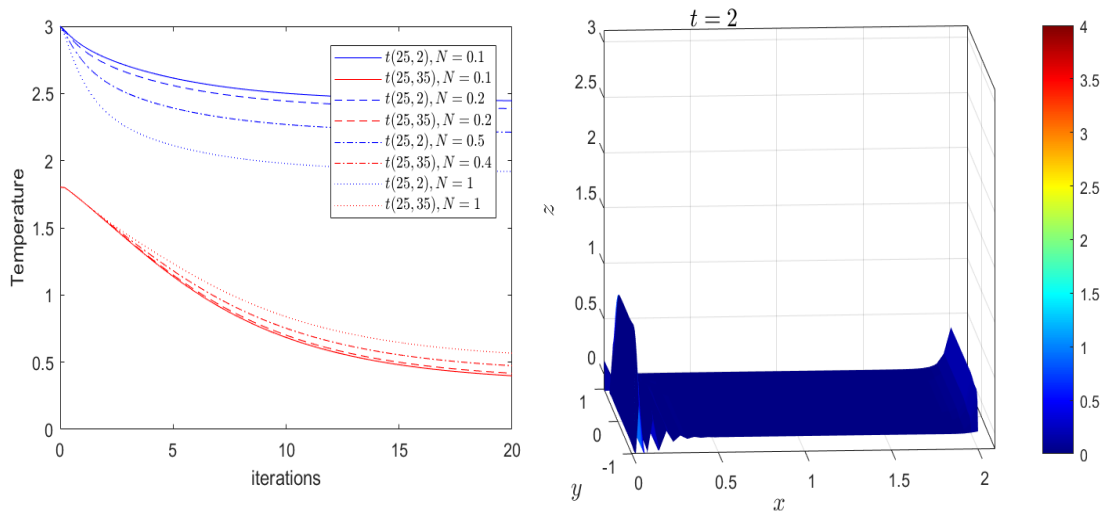


Figure 12 - Impact of N on motion equation for different values with $t= 0 – 20$.

4. Conclusions

In this section, because of the occurrence of effects on the tested equations, we have presented some of the results obtained from the calculation done on equations (12) and (14) for different places in the region of solution. Figures 2-12 show several results. In terms of the energy equation, we can see that the higher the Brinkmann number, the Bouger number, the Prandtl number, and the relative temperature, the closer we get to stability, as shown in Figures 2, 5, 6, and 7. The effect of Hartmann number M is diverging from the stability for both of the motion and energy when M and temperature are increasing. As illustrated in Figures 4 and 8, the greater the Reynolds, the closer to stability are both equations (motion and energy). According to Figure 9, the higher the magnetic Reynolds number, the farther the system from stability. Figures 11 and 12 indicate that the closer the motion equation gets to stability, the smaller Hartmann number and the new physical quantity N .

Acknowledgement

The authors are very thankful to the University of Mosul, College of Pure Science Education for its facilities, which have helped to enhance the quality of this work.

References

- [1] W. S. Khudair and G.S. Dheia Al-khafajy. "Inuence of heat transfer on Magnetohydrodynamics oscillatory ow for Williamson fluid through a porous medium", *Iraqi Journal of Science*, vol. 59, pp. 389397, 2018.
- [2] T. Mehta, et al. "Oscillatory fluid ow and heat transfer through porous medium between parallel plates with inclined magnetic field, RADIATIVE HEAT FLUX AND HEAT SOURCE", *International Journal of Applied Mechanics and Engineering*, vol.25, pp.88-102, 2020. DOI: 10.2478/ijame-2020-0022.
- [3] G.S. Dheia, et al. "Radiation and Mass Transfer Effects on MHD Oscillatory Flow for Jeffery Fluid with Variable Viscosity Through Porous Channel in the Presence of Chemical Reaction", *Science International Lahore*, 2nd SICAPM, vol. 31, pp. 27-28, 2019.
- [4] R. Hanvey , et al. "MHD Flow of Incompressible Fluid through Parallel Plates in Inclined Magnetic field having Porous Medium with Heat and Mass Transfer", *International Journal of Scientific and Innovative Mathematical Research IJSIMR*, vol. 5, pp. 18-22, 2017.
- [5] M. Sheikholeslami, et al. "Steady nanouid ow between parallel plates considering thermophoresis and Brownian effects", *textsl Journal of King Saud University Science*, vol. 28, pp. 380-389, 2016.
- [6] T. Mehta, et al. "Oscillatory fluid ow and heat transfer through porous medium between parallel plates with inclined magnetic field, RADIATIVE HEAT FLUX AND HEAT SOURCE", *International Journal of Applied Mechanics and Engineering*, vol.25, pp.88-102, 2020. DOI: 10.2478/ijame-2020-0022.
- [7] S. Mukhopadhyay and I.C. Mandal . "Magneto hydrodynamic (MHD) mixed convection slip ow and heat transfer over a vertical porous plate", *Engineering Science and Technology an International Journal*, vol.18, pp. 98-105, 2015.
- [8] K. Kumari and M. Goyal .. "Heat and Mass Transfer Flow of MHD Viscous Dissipative Fluid in aChannel with a Stretching and Porous Plate", *An International Journal of Applied Mathematics and Information Sciences Letters*, vol.5, pp. 81-87, 2017.
- [9] K. Jabr and A. Ahmed. "Inuence of MHD on Steady State Newtonian Fluid Flow in a Vertical Channel with Porous Wall using HAM", *Iraqi Journal of Science*, vol.55, pp.811-821, 2014.
- [10] M. F. Mosa. 1979. "Radiative Effect in Magneto-Fluid Dynamic Channel Flow", Ph. D. Thesis, University of Bradford March.
- [11] A. Hammodat and H. Saleem. "Numerical Solution of Electromagnetic Problem in Horizontal Porous Medium", *ITALIAN JOURNAL OF PURE AND APPLIED MATHEMATICS*, 2020.
- [12] B. Carnhan, et al. *Applied Numerical Methods*. textslJohn Wiely and Sons, INC. NewYork.London. Sydney.Toront, 1969.
- [13] G. D. Smith. *Numerical Solution of Paryial Differential Equations. Finite Difference Methods, third edition*, 1985.